

Andrew M. Baker

## Contents

Introduction .....	340
Basic Bone and Fracture Histology .....	340
Bone Structure .....	340
Bone Formation .....	342
Fracture Healing .....	343
Handling Bones .....	344
The Classic Metaphyseal Lesion (CML) .....	346
Rib Fractures .....	350
Skull Fractures .....	357
Mimics of Abuse .....	358
Recommendations .....	364
Conclusions .....	372
Bibliography .....	372

---

## Abstract

Examination of the skeletal system of the deceased child, particularly in cases where physical abuse may have occurred, is a critical part of the postmortem examination. Since some injuries, particularly metaphyseal injuries, would not be discernible with a traditional autopsy approach, radiographic imaging of the deceased child is critical. The presence of healing fractures in the setting of fatal visceral trauma may distinguish a single acute event from a pattern of inflicted injury (“battered child syndrome”). Though many pathologists may have little experience handling or interpreting bony injuries, most bony findings are readily

---

A.M. Baker  
Hennepin County Medical Examiner’s Office, Minneapolis, MN, USA  
e-mail: [andrew.baker@co.hennepin.mn.us](mailto:andrew.baker@co.hennepin.mn.us)

removed at autopsy and can be decalcified and subjected to histological evaluation with very little investment in special techniques or tools. Correlation of the radiographic, gross, and microscopic findings is invaluable to the radiologist, pediatrician, and pathologist alike.

---

## Introduction

The importance of confirming or refuting the presence of fractures in the deceased infant or young child cannot be overemphasized. Because fractures are often present in the extremities and/or lack corresponding external evidence of injury, radiography in the deceased child is critically important if such fractures are to be found.

When radiographs are negative for bony injury, they:

- Provide assurance to family, friends, and caretakers.
- Provide an extra measure of comfort to the pathologist.

When radiographs are positive for bony injury, they:

- Guide the pathologist to areas not normally examined.
- Effectively rule out the diagnosis of sudden infant death syndrome (SIDS).
- Provide graphic demonstration of injury.

Why bother finding fractures?

- In most cases, fractures are evidence of trauma.
- Quality evaluation of fractures by the pathologist facilitates radiological–pathological correlation; in some cases, it may confirm or refute inconclusive radiographic findings.
- Fracture evaluation can confirm the multiplicity and/or chronicity of injuries.
- Histological evaluation can assist with the assessment of the stage of healing.
- Histological evaluation may assist in confirming or refuting underlying diseases or conditions.
- Some fractures have a very high specificity for inflicted injury.

The traditional autopsy is an excellent tool for finding external, visceral, cerebral, and ocular injuries. While some bones (e.g., the skull, ribs, parts of the spine, parts of the pelvis) can be examined grossly, the autopsy is limited in its ability to detect injuries of the extremities in the infant and small child (Figs. 15.1–15.3).

---

## Basic Bone and Fracture Histology

### Bone Structure

*Compact bone* makes up the cortex, where there is little soft tissue. *Cancellous bone* makes up the central region (medulla), where spicules of bone are admixed

**Fig. 15.1** Fractures in infants can be categorized by their specificity for abuse. Fractures highlighted in *blue*, without the use of radiographs, would be very difficult to find in a standard autopsy

### Specificity of Infant Fractures for Abuse\*

High	Moderate	Low
<ul style="list-style-type: none"> <li>• Ribs (especially posterior)</li> <li>• <b>Metaphyseal</b></li> <li>• <b>Scapula</b></li> <li>• <b>Spinous process</b></li> <li>• Sternum</li> </ul>	<ul style="list-style-type: none"> <li>• Multiple</li> <li>• Different ages</li> <li>• <b>Epiphyseal</b></li> <li>• Vertebral body</li> <li>• <b>Digital</b></li> <li>• Complex skull</li> </ul>	<ul style="list-style-type: none"> <li>• <b>Subperiosteal new bone</b></li> <li>• Clavicle</li> <li>• <b>Long bone shaft</b></li> <li>• Linear skull</li> </ul>

\*adapted from Kleinman, 1998

**Fig. 15.2** A “babygram” is inadequate for finding subtle skeletal injuries, particularly of the extremities. In this “babygram,” for example, no comment can be made about the metaphyses of the right elbow



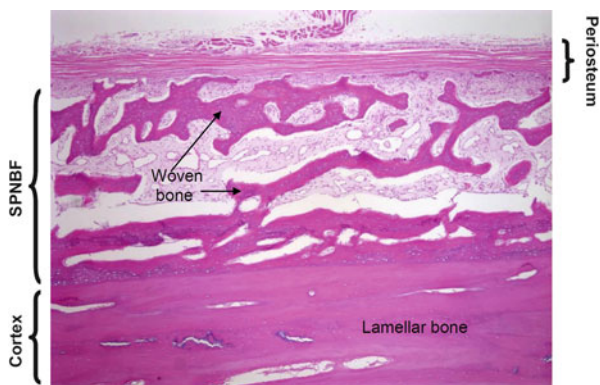
with soft tissue. At the microscopic level, one can distinguish lamellar bone (regularly arranged sheets) and woven bone (an irregular feltwork). *Lamellar bone* predominates in areas of slow growth and remodeling, and deposition of lamellar bone requires a preexisting lattice of woven bone or lamellar bone. *Woven bone* predominates in areas of rapid bone growth, including embryonic bone, Codman’s triangle, tumor bone, and fracture callus. While woven bone is flexible and allows rapid mineralization, bone formation, and bone resorption, it is also less rigid and has less strength than lamellar bone.

*Periosteum* surrounds the bony cortex except in articular cartilage. Periosteum has two layers: the outer fibrous layer and the inner cellular (cambium) layer. Sharpey’s fibers anchor periosteum and tendons to bone. These fibers are less developed in children, and fractures of children’s bone often result in fraying or displacement,



**Fig. 15.3** A complete pediatric skeletal survey with collimated views of the long bones, akin to that which is performed on living children suspected of having been abused, is strongly recommended in deceased infants and small children. In this radiograph, for example, the metaphyses and diaphyses of the long bones of the right arm are clearly visualized

**Fig. 15.4** Bony cortex of the ulna of a fatally battered 8-week-old. The normal cortex and periosteum are separated by subperiosteal new bone formation (SPNBF), and the appearances of woven bone and lamellar bone are readily distinguished (Hematoxylin and Eosin, H&E  $\times 20$ )



rather than actual breaking of the periosteum. Subperiosteal new bone formation (SNBF) in children is a sequel of periosteal–cortical separation, occurring in response to hemorrhage beneath the periosteum and is often readily visible on radiographs. In adults, the periosteum is firmly adherent due to Sharpey’s fibers, with the periosteum tending to break at the bony fracture site (Fig. 15.4).

### Bone Formation

Enchondral and intramembranous formation are the two mechanisms of bone embryogenesis in humans. In *enchondral bone formation*, bone replaces

a preexisting cartilaginous model. This occurs in the long bones: ribs, vertebrae, and extremities. Eventually, the only continuous enchondral growth occurs at the physis. In *intramembranous bone formation*, progenitor cells organize into trabeculae, differentiate into osteoblasts, and form trabeculae of woven bone. It is upon these trabeculae of woven bone that lamellar bone is then placed. Bone growth occurs via inner resorption and outer apposition of new bone. Intramembranous growth occurs in the flat bones of the skull and face. Fracture healing is essentially the process of bone regeneration, recapitulating embryonic intramembranous bone formation.

## Fracture Healing

The stages of fracture healing may be divided into four broad ranges: inflammation and induction, soft callus, hard callus, and remodeling.

*Inflammation and induction* spans the time from injury to the appearance of new bone. This stage consists of two competing processes: osteolytic activity along with removal of hemorrhage and dead tissue and deposition of granulation tissue, fibrous tissue, and osteoid. The lysis taking place within the fracture site explains the radiolucency often appreciated on radiographs. When examining fractures under the microscope, the pathologist must take care not to interpret the resorption of normal bone adjacent to a fracture as evidence of bony dysplasia.

*Soft callus* is thought to begin at about 10–14 days post-injury in older children and probably earlier in infants. New woven bone and cartilage are laid down, with the woven bone gradually maturing into trabeculae. The progenitor cells entering the fracture site are actually pluripotent and can differentiate into osteoblasts (producing osteoid), chondroblasts (producing cartilage), or fibroblasts (producing fibrous tissue). The predominant pathway taken depends on how well immobilized and oxygenated the fracture site is. Unlike many animal models, a callus composed largely of cartilage is not the preferred route in humans. The soft callus stage usually lasts about 3–4 weeks. At the end of the stage the ends of bony fragments are no longer easily moved, and there is obliteration of the radiographic fracture line.

In the *hard callus* stage, both periosteal callus (outside the bone cortex) and endosteal callus (inside the bone cortex) are converted to lamellar bone. Nearly all of the hematoma, inflammation, and necrotic tissue have been removed from the fracture site, although it should be noted that histologically, the healing of the endosteal portion of a fracture may lag far behind the periosteal portion. At the end of the hard callus stage, the fracture is now radiographically solidly united.

The goal of *remodeling* is complete restoration of the medullary cavity and the cortex. While this might never occur completely in some adult fractures, in children it may occur despite wide displacement or angulation of the fracture (Figs. 15.5–15.15).

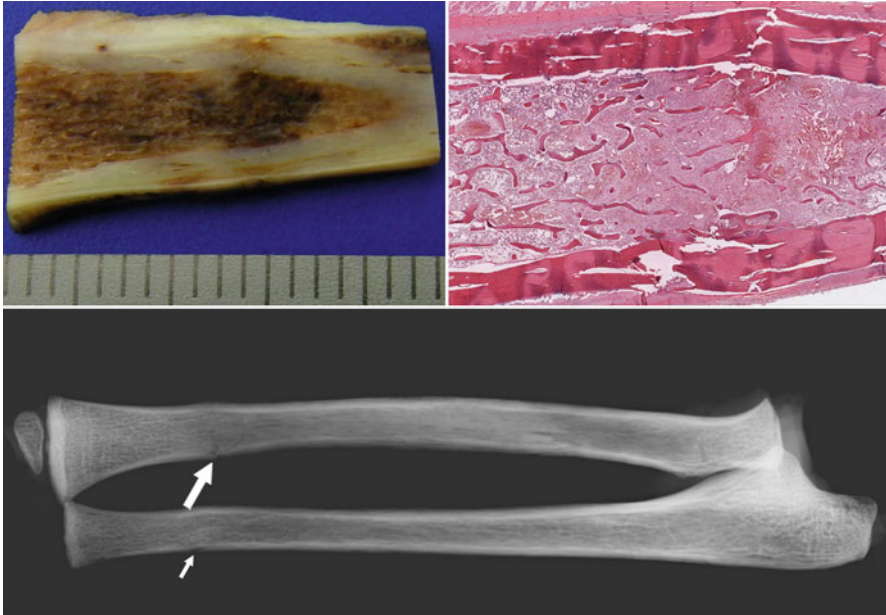


**Fig. 15.5** Distal radius (*large arrow*) and ulna (*small arrow*) fractures in a battered 3-year-old. These would have been completely undetected clinically and at autopsy without a skeletal survey. The gross (*upper left*) and microscopic (*upper right*) images are the radial fracture (Hematoxylin and Eosin, H&E ×10)

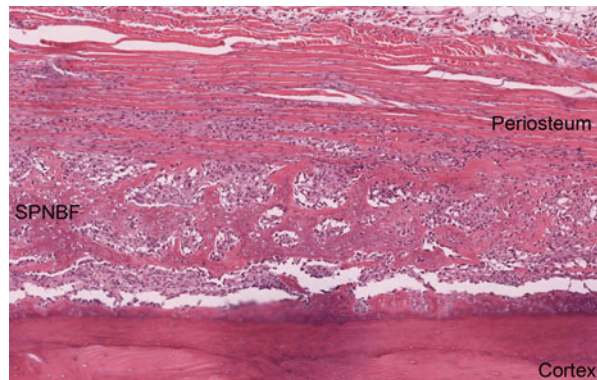


**Fig. 15.6** SPNBF associated with the radial fracture shown in Fig. 15.5 (Hematoxylin and Eosin, H&E ×20)

## Handling Bones

When bony injuries (or apparent bony abnormalities) are detected radiographically, it is usually best to resect the bone in question as well as the



**Fig. 15.7** The endosteal (medullary) part of the callus from the radius in Fig. 15.5 consists largely of granulation tissue and loose mesenchyme (*black arrow*); however, islands of very early osteoid (*red arrows*) are ringed by osteoblasts (Hematoxylin and Eosin, H&E  $\times 200$ )

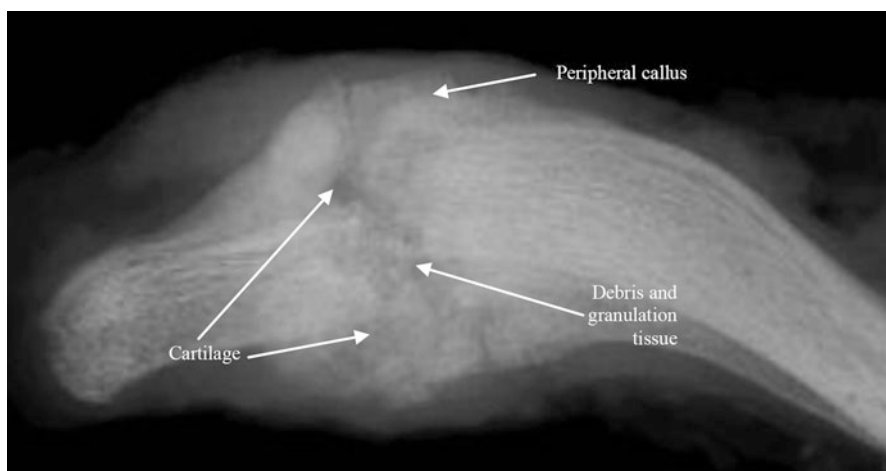
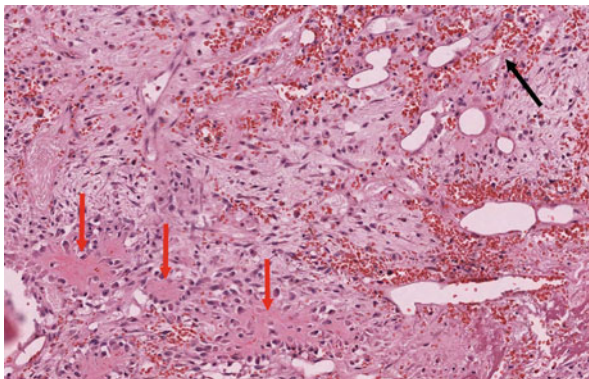


**Fig. 15.8** Radiograph of a healing clavicle fracture found in a deceased infant. Features that correspond to the histology (Fig. 15.9) are highlighted

contralateral normal bone if possible for a control. Resected specimens should then be reradiographed, before or after fixation, but before decalcification. Larger specimens often produce very nice post-resection radiographs if they are bivalved. A small wet tile saw (if available) or a hand held coping saw works well for this. In the event that multiple contiguous posterior rib fractures are present, these are best resected en bloc with the corresponding vertebral bodies and contralateral posterior ribs. After fixation, the rib–vertebra–rib complexes can be separated one by one and reradiographed in the axial plane (Figs. 15.16–15.19).

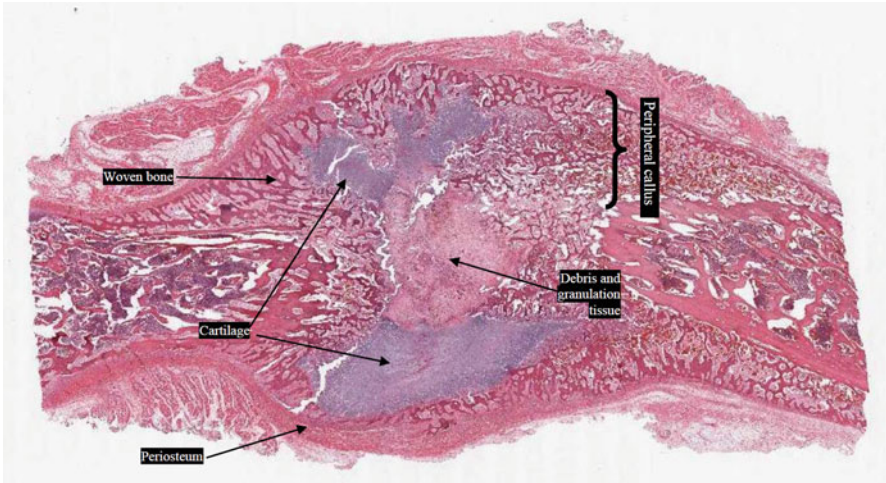


**Fig. 15.9** Whole-mount histology of the healing clavicle fracture radiographed in Fig. 15.8 (Hematoxylin and Eosin, H&E  $\times 1$ )



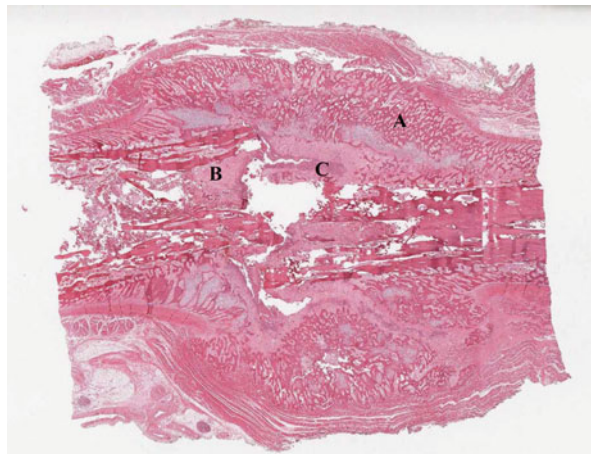
**Fig. 15.10** Gross appearance of a radial fracture in a fatally abused 13-month-old

## The Classic Metaphyseal Lesion (CML)

Of all the fractures described in child abuse, none appears more specific than the metaphyseal fracture, first described by the pediatric radiologist John Caffey. Injuries corresponding to CMLs were not reported in Caffey's landmark paper (1946) that described subdural hematomas and long bone fractures in infants. It was not until 1957 that Caffey introduced the terms "bucket handle" and "corner fracture" to describe the radiographic appearance of CMLs (Caffey 1957). Caffey believed that these lesions were the result of avulsion of peripheral metaphyseal



**Fig. 15.11** Low power microscopy of the fracture in Fig. 15.10. Areas A, B, and C are discussed in Fig. 15.12 (Hematoxylin and Eosin, H&E  $\times 1$ )



fragments at the point of periosteal insertion. However, subsequent postmortem studies of these lesions have shown them to be more extensive than is generally appreciated radiographically (Kleinman 2008).

Kleinman et al. introduced the term *classic metaphyseal lesion* (CML) to describe the injury. CMLs are the most frequently encountered long bone injuries in infants dying with evidence of abuse. CMLs are highly specific for abuse, although they are observed in half or fewer of cases. CMLs most often occur in the distal femur, proximal tibia, distal tibia, and proximal humerus and are seen almost exclusively in children less than 2 years old. The lesion is a series of microfractures across the metaphysis, roughly parallel to the physis, although it may not travel the entire width of the bone. The long-term sequelae of CMLs appear to be minimal. Rarely, CMLs have been described in settings other than abuse, such as in accidents, cesarean sections, small premature infants, infants with rickets who undergo a vigorous passive range of motion exercises, and during physical therapy or orthopedic manipulation for club foot. Metaphyseal irregularity and fragmentation have been described in a variety of skeletal dysplasias, although the diagnosis generally becomes clearer when viewed in the context of clinical and additional radiological findings. Follow-up skeletal imaging will generally show no change in such metaphyseal fragments, in contrast to the healing of the CML (described below) (Kleinman 2008, 2009).

The work of Kleinman et al. documented the histological appearance of the CML as a series of microfractures in the subepiphyseal region of bone. This region is the primary spongiosa, and it is the most immature area of the mineralized matrix in the growing metaphysis. When complete, the fracture fragment may be conceptualized as a wafer or disk of bone separated from the shaft by the series of metaphyseal microfractures. The CML, when complete, is a disk with a broad, thin center and a thick circumferential rim. Centrally, the fracture abuts the chondro-osseous junction and peripherally tends to turn away from the physis to undercut the subperiosteal bone collar (Kleinman et al. 1986; Lonergan et al. 2003).

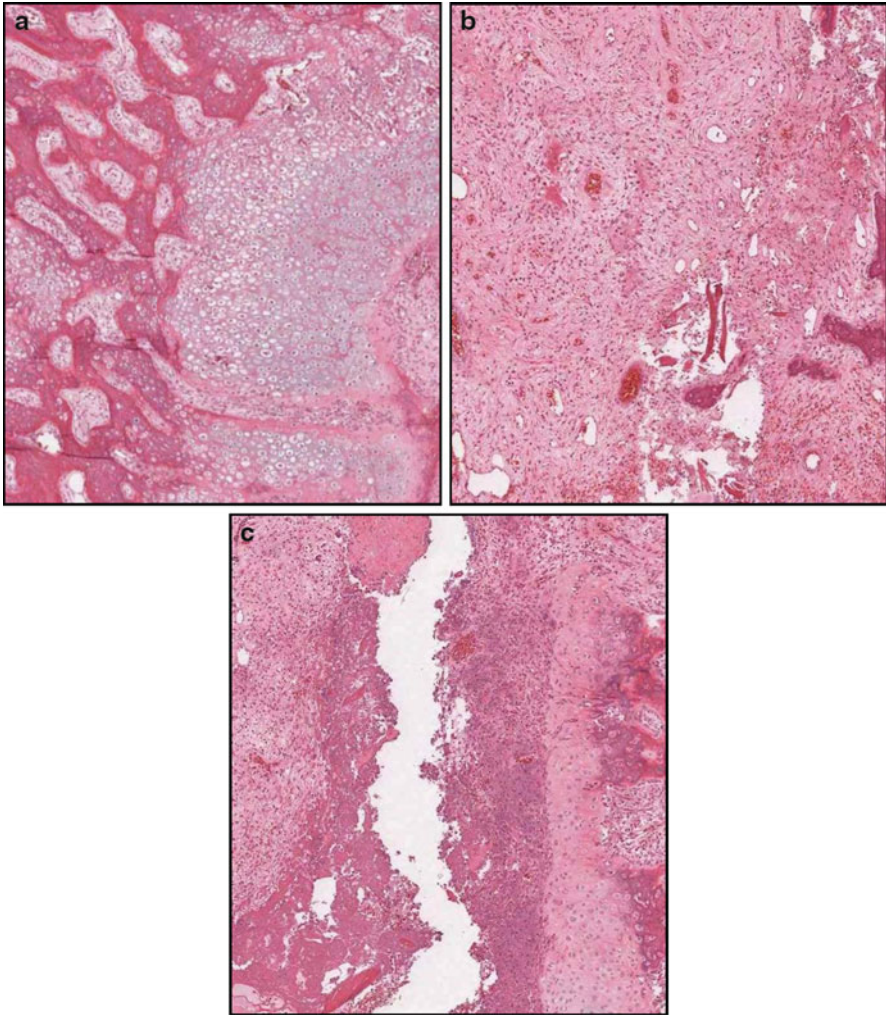


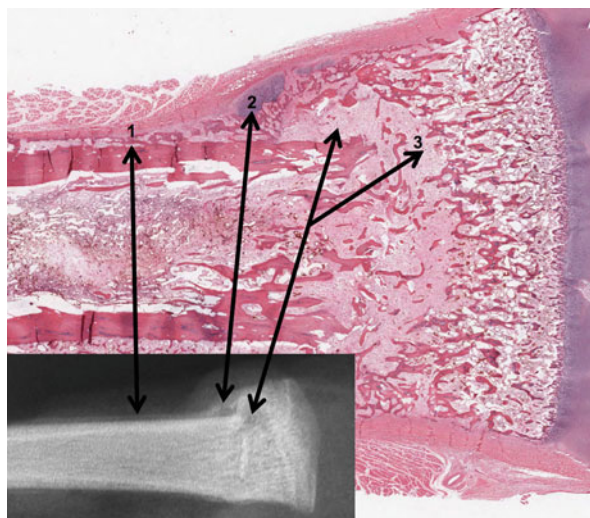
**Fig. 15.12** Higher power microscopy of the areas labeled in Fig. 15.11. The periphery of the fracture callus (a) is composed of cartilage and woven bone (with very early lamellar bone), while the central part of the callus consists of granulation tissue (b) and persistent necrotic debris (c). When assessing “age” of the fracture, one must look at the whole fracture and not just selected areas. In most instances, the healing of the central part of the callus will lag far behind the periphery (Hematoxylin and Eosin, H&E a, b  $\times 40$ ; c  $\times 20$ )

There is typically minimal or no periosteal disruption and little or no callus formation. However, changes at the physis subjacent to a CML may indicate a subacute CML. The normal physis is a disk of chondrocytes that extends in columns toward the metaphysis. Uninjured regions of the metaphysis–physis

**Fig. 15.13** Gross photograph of a distal radius fracture in a fatally abused 15-month-old



**Fig. 15.14** The radiographic features of the fracture (*lower left inset*) from Fig. 15.13, such as SPNBF (1), cartilage in the fracture periphery (2), and granulation tissue in the central callus (3), are clearly demonstrated histologically (Hematoxylin and Eosin, H&E  $\times 20$ )



complex will grow and mineralize normally around the fractured area; however, the area distal to the CML does not mineralize normally, resulting in the chondrocytes of the physis persisting abnormally. Histologically, this pattern appears as an area of hypertrophic chondrocytes (Kleinman et al. 1991).

When an x-ray beam is perpendicular to the long axis of the metaphysis, the comparatively thicker ends of the metaphyseal lesion appear as relatively discrete, triangular bony fragments, hence the term “corner fracture.” When the x-ray beam is angled relative to the long axis of the metaphysis, the appearance resembles a “bucket handle.” The two terms refer to the same injury, with the appearance of the injury depending on the radiographic projection. Contusions overlying CMLs are often absent. Precise dating criteria are not published, though Kleinman (1998, 2008) suggests that most healing CMLs become radiographically inconspicuous at 4 weeks and completely healed at 6 weeks (Figs. 15.20–15.29).



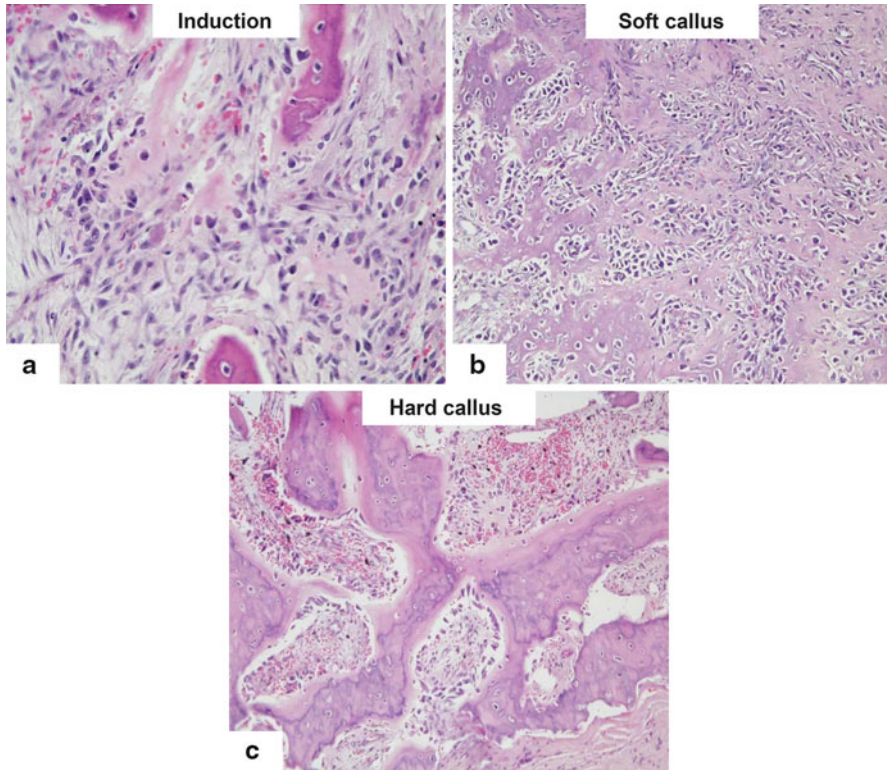


**Fig. 15.15** (a–c) Three (of 52) rib fractures in a fatally battered 7-week-old. The fractures are in various stages of healing, as illustrated by the early organization of osteoblasts into trabeculae, with osteoid production (a); formation of mineralizing trabeculae of woven bone (b); and mineralized trabeculae of woven bone upon which lamellar bone is being deposited (c). a, b, and c represent the “oldest” areas in three different fractures (Hematoxylin and Eosin, H&E a  $\times 200$ ; b, c  $\times 100$ )

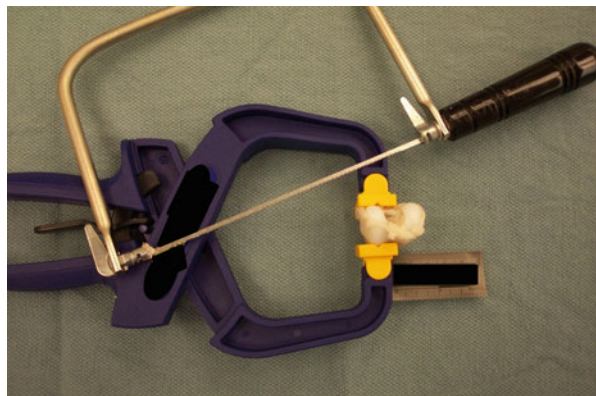
## Rib Fractures

In older children and adults, rib fractures occur as a result of recognizable trauma such as motor vehicle accidents and falls. Outside the setting of abuse, rib fractures are distinctly unusual injuries in infants. Rib fractures are the most common fractures found in infants dying from inflicted injury. A very tight hold around the infant chest by adult hands generates a squeezing force on the immature skeleton and may result in fractures of the anterior, lateral, and posterior aspects of the rib. In rare cases, rib fractures (including posterior rib fracture) have been reported as a result of birth trauma. In a large series of children admitted to a major medical center for trauma, the positive predictive value of a rib fracture as an

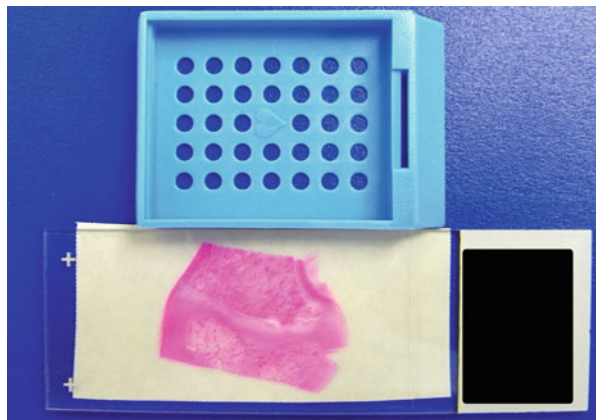
**Fig. 15.16** Numerous bones can be placed on a single x-ray film. Radiography of resected bones often provides more detail than the original skeletal survey



**Fig. 15.17** Bisecting larger specimens will improve fixation and can be accomplished with fairly inexpensive tools



**Fig. 15.18** Most infant and small child bony abnormalities (such as the metaphyseal lesion in this proximal humerus) can readily fit into standard histology cassettes when appropriately decalcified and trimmed



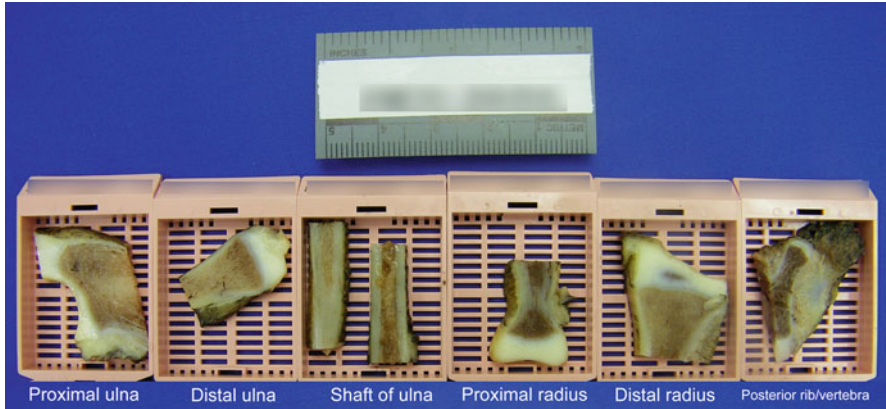


**Fig. 15.19** Multiple bones (some injured, some normal controls in this case from a fatally abused 3-year-old) can be readily processed for routine histology in standard cassettes after decalcification



**Fig. 15.20** Gross appearance of the normal distal femur from a 16-week-old

indicator of nonaccidental injury in children younger than 3 years of age was 95 %; this increased to 100 % when other causes were excluded by historical and clinical circumstances (Barsness et al. 2003).

Maguire et al. (2006) published a review on cardiopulmonary resuscitation (CPR) and rib fractures spanning the medical literature from 1950 to 2005. They concluded that rib fractures related to CPR (three of 923 children) were most likely to be anterior and could be multiple. They did not find posterior rib fractures related to CPR, noting



**Fig. 15.21** Histology of the normal distal femoral physis photographed in Fig. 15.20. The chondrocytes mature from resting (*R*) to proliferating (*P*) to hypertrophying (*H*) in the epiphysis (*Ep*) and then mineralize (*M*) in the metaphysis (*Me*) (Hematoxylin and Eosin, H&E  $\times 40$ )

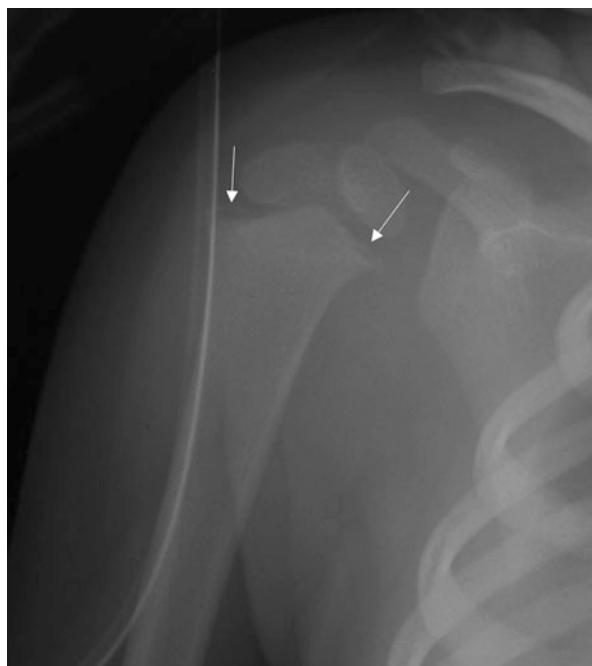
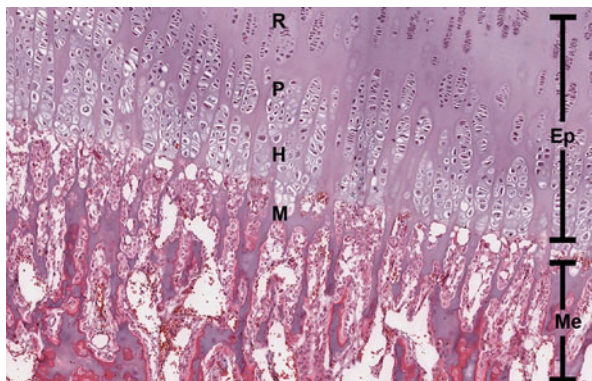


**Fig. 15.22** The radiograph depicts a proximal humeral metaphyseal fracture (*arrows*) in a fatally battered 15-month-old. Note the “bucket handle” appearance

“sound biomechanical reasons for this.” They did note that weaknesses in the literature were likely related to the degree to which rib fractures were actually being sought, radiographically and/or at autopsy.

A recent study by Dolinak (2007) suggests that anterolateral fractures from CPR may be more common in infants than previously appreciated; such fractures would not be expected to be visible on radiographs. In this study, 8 of 70 deceased infants with no autopsy or historical evidence of injury were found to have anterolateral rib

**Fig. 15.23** The low power microscopy of the humerus in [Fig. 15.22](#) shows the metaphyseal fracture (*arrows*) spanning the width of the physis (Hematoxylin and Eosin, H&E  $\times 1$ )

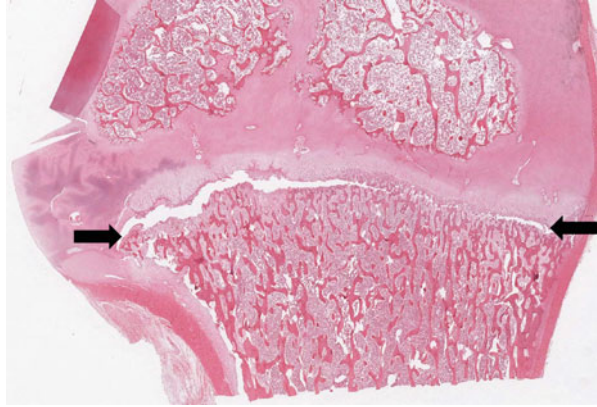


**Fig. 15.24** Granulation tissue with osteoclastic activity (*arrows*) in the fracture site from [Fig. 15.22](#) (Hematoxylin and Eosin, H&E  $\times 200$ )

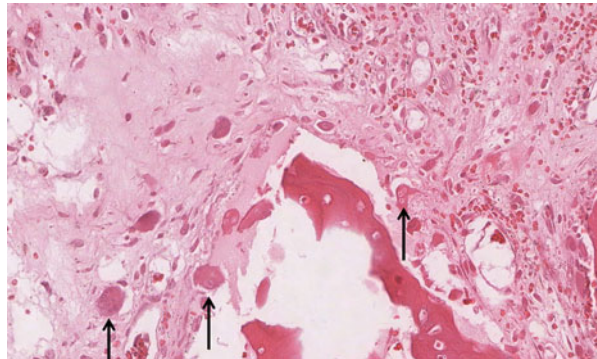


**Fig. 15.25** Abnormal persistence of hypertrophied chondrocytes, forming billowing islands of cartilage that protrude into the fracture site from [Fig. 15.22](#) (Hematoxylin and Eosin, H&E  $\times 200$ )

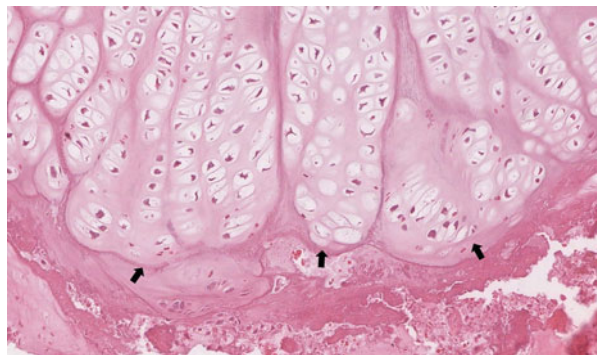




**Fig. 15.26** Bilateral proximal tibia CMLs in a fatally abused 4-month-old. Note the “bucket handle” appearance (*arrows*)

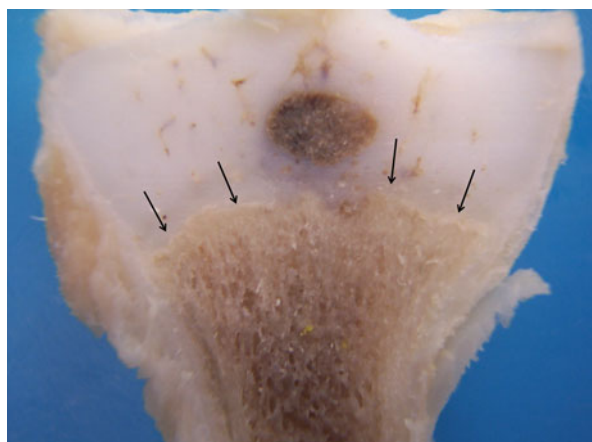


**Fig. 15.27** Gross appearance of a proximal tibia CML from the radiograph in [Fig. 15.26](#). Note the ragged, moth-eaten appearance of the metaphysis (*arrows*) compared to the normal metaphysis in [Fig. 15.20](#)

fractures. Most of these involved multiple ribs, in many instances bilateral. In all cases, the fractures were noted to be “subtle,” with “little if any associated blood extravasation,” and “would have been easily missed had the parietal pleura not been stripped.”

Clouse and Lantz, in work presented in [2008](#), described four cases of hospitalized neonates and infants who were found to have posterior rib fractures apparently related to CPR performed in accordance with current American Heart Association recommendations for infants (thumbs on the sternum with the fingers encircling the chest and back). Three of their cases were classified as

**Fig. 15.28** Whole-mount appearance of the CML depicted in Fig. 15.27. The fracture spans the width of the metaphysis (*arrows*) (Hematoxylin and Eosin, H&E  $\times 1$ )

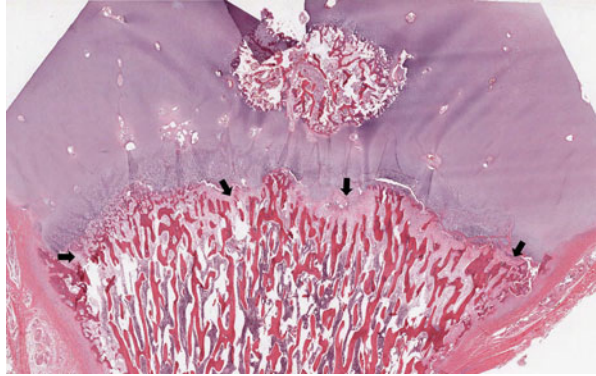
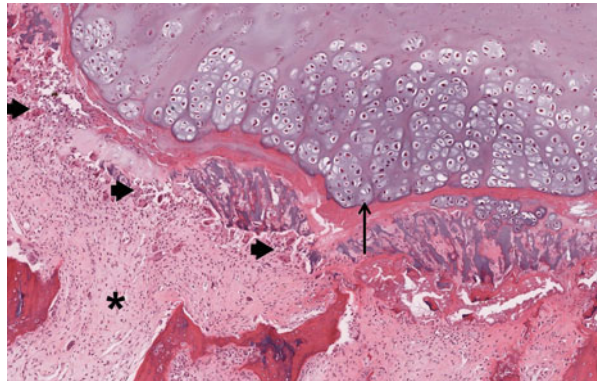


**Fig. 15.29** Microscopy of the CML in Fig. 15.27. Reactive tissue changes (*\**), abundant osteoclasts (*arrowheads*), and billowing islands of persistently hypertrophied chondrocytes (*arrow*) are seen (Hematoxylin and Eosin, H&E  $\times 100$ )



acute fractures; one case had evidence of healing ascribed to prior episodes of CPR. Though noting that rib fractures in small children are most commonly the result of nonaccidental injury, the authors wisely point out that such injuries must be interpreted in the context of “a complete autopsy and a thorough investigation of the circumstances of death.” Duval and Andrew reported a case in 2007 in which posterior rib fractures, presumably related to this method of CPR, were found in a previously healthy 47-day-old.

Weber et al. (2009), in a series of 546 postmortem examinations for sudden unexplained infant deaths, found rib fractures in 24 cases. In 15 cases the fractures were healing, and 10 of the 15 cases had other physical findings considered due to nonaccidental injury. Of the nine cases in which the fractures appeared fresh, all of the fractures were anterolateral, and in seven of the nine cases, there were no other physical findings to suggest trauma. Though all seven of the cases remained “undetermined” in manner, this latter group of rib fractures was regarded as

resuscitation-related. The authors also point out that while 93 % of the healing rib fractures were demonstrable on routine radiographic skeletal surveys, only 22 % of the fresh fractures were identified this way.

More recently, Matshes and Lew (2010) described rib fractures in five deceased infants who had received two-handed CPR as described above. All of the fractures, which ranged from as few as two and unilateral to nine and bilateral, were noted to be on the anterolateral arc and minimally displaced, with only subtle associated gross hemorrhage. No posterior rib fractures were found. Interestingly, none of the fractures was identified on primary radiographic screening, and in only one case were fractures even suggested on rescreening.

Different mechanical forces are exerted on different parts of the rib cage when an infant is squeezed around the chest. Posteriorly, the ribs are attached to the vertebral bodies and transverse processes. As the ribs are squeezed, the posterior rib arc is levered over the transverse process, resulting in ventral (and sometimes complete) cortical disruption. Squeezing creates both anterior and posterior compressive forces laterally, resulting in buckling of the inner cortex and distraction of the outer cortical fracture margins. Sternal compression produces inward bending of the anterior costochondral junction, leading to fracture (Kleinman et al. 1992, 1996; Kleinman and Schlesinger 1997).

Acute fractures of the rib are characterized by disruption of the cortex and subjacent bony trabeculae. Hemorrhage is often observed at the fracture site. Radiographically, acute rib fractures may be quite difficult to discern, especially if the fracture is incomplete, nondisplaced, and viewed in an area with many superimposed structures or if the fracture line is oblique to the x-ray beam. Fractures of the costovertebral articulation are particularly difficult to appreciate radiologically for all of these reasons (Kleinman et al. 1988). Such acute fractures are optimally visualized with computed tomography (CT) scanning, although this may be unavailable to most pathologists autopsying infants pronounced dead before such radiographic evaluation could occur. With healing, most fractures become more visible on radiographs, as subperiosteal new bone and callus become evident (Figs. 15.30–15.49).

---

## Skull Fractures

Skull fractures in infants and small children can be the result of abuse, accidental falls, and other forms of trauma. Although some types of skull fractures (complex, multiple, diastatic) may be more common in inflicted injury than in accidental injury, no skull injury pattern is diagnostic of abuse. The radiographic and histological appearance of healing skull fractures differs from most other fractures in that there is very little subperiosteal reaction and little (if any) formation of endosteal or periosteal callus (Rao and Carty 1999). Skull fractures may remain radiologically detectable for several months after the injury.



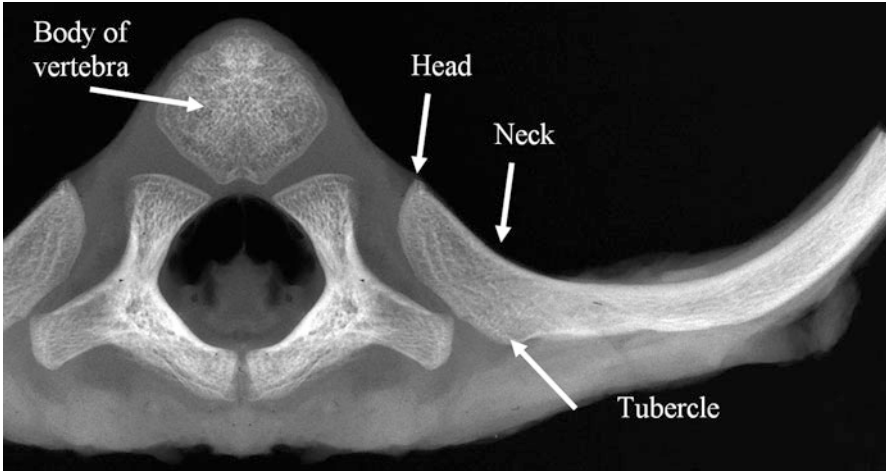


**Fig. 15.30** Radiograph of a resected vertebral body with the posterior arcs of the ribs (normal infant)

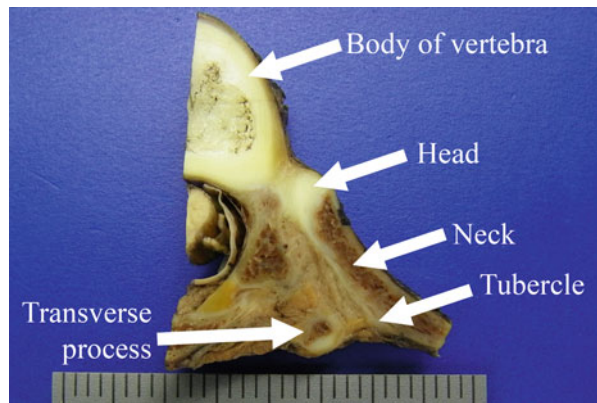


**Fig. 15.31** Gross appearance of the normal posterior rib-vertebral articulation from a 3-year-old

Microscopically, the healing skull fracture may consist largely of fibrous tissue, without the production of osteoid or cartilage. For all of these reasons, very little can be said about the age of a skull fracture other than that it is healing (Fig. 15.50).

## Mimics of Abuse

A variety of disease processes may account for unexplained fractures in infancy (Bishop et al. 2007). Although an exhaustive discussion of entities that can



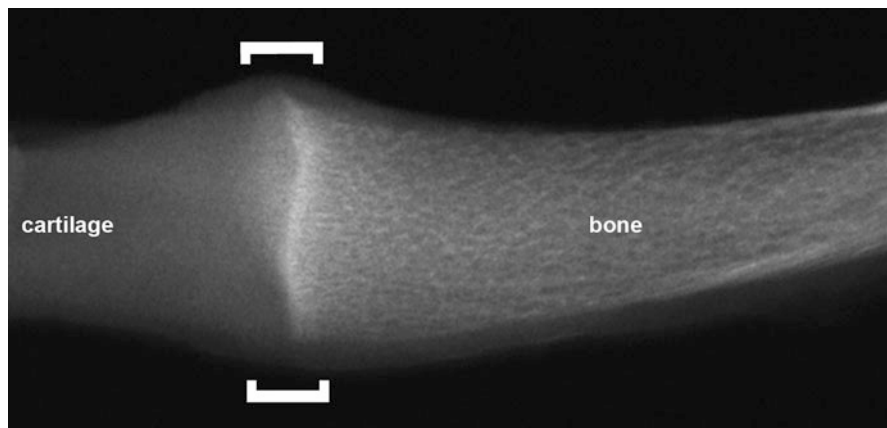


**Fig. 15.32** Radiograph of a normal infant costochondral junction illustrating bone, cartilage, and the chondro-osseous junction (*brackets*)

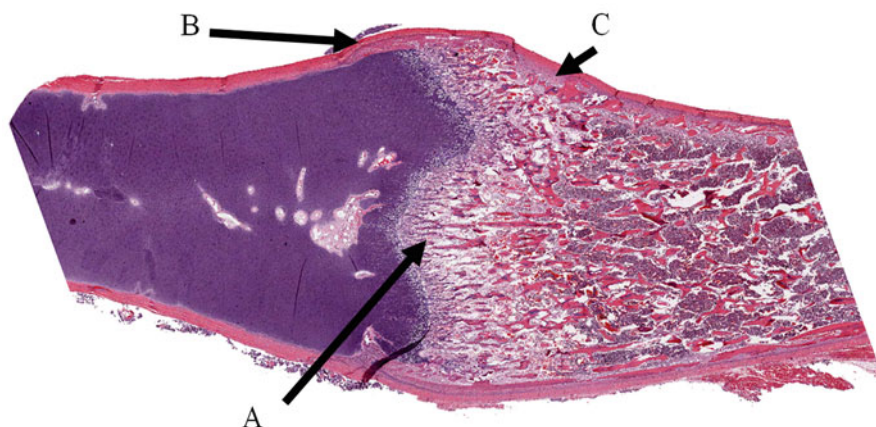


**Fig. 15.33** Whole-mount microscopy of a normal infant chondro-osseous (costochondral) junction. Specific features (A, B, C) are described in Fig. 15.34a-c (Hematoxylin and Eosin, H&E  $\times 1$ )

predispose to or mimic fractures is beyond the scope of this text, three commonly posited entities warrant further discussion here: “temporary brittle bone disease” (TBBB), subclinical vitamin D deficiency, and osteogenesis imperfecta.

First proposed by Paterson in 1993 and further described by Miller (Miller 1999, 2003; Miller and Hangartner 1999), TBBB is purportedly a self-limited condition that mimics abusive skeletal injury because there are multiple fractures with denial of harm to the child, there are no reported episodes of trauma, no other internal or external injuries are found, and there is no radiographic or laboratory evidence of metabolic or genetic bone disease. While the *concept* that there

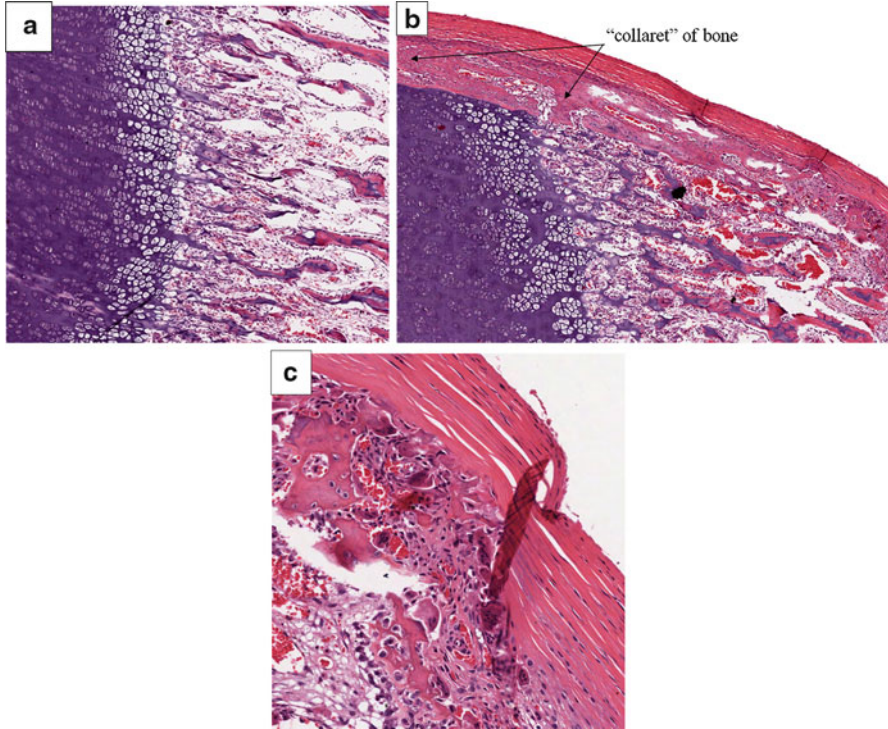


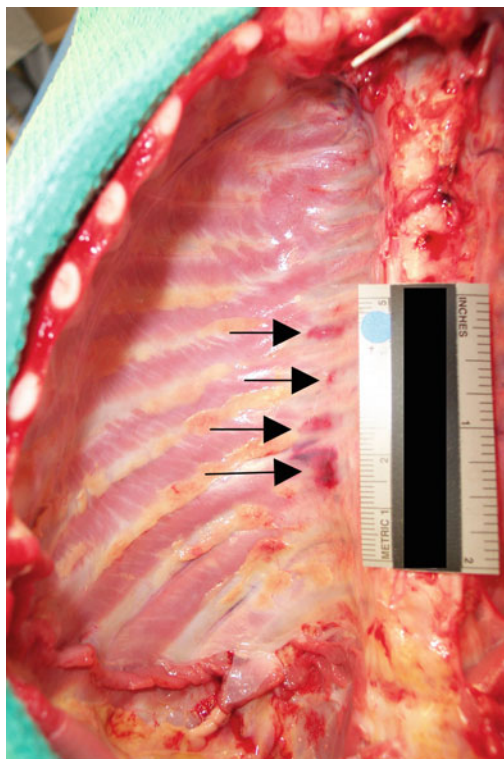
**Fig. 15.34 (a–c)** The metaphysis of the normal infant costochondral junction looks like the metaphysis of any growing long bone (a). A “collaret” of bone typically surrounds the chondro-osseous junction (b). The cortex near the chondro-osseous junction often appears osteopenic due to the remodeling and “cutback” that takes place during longitudinal growth (note the numerous osteoclasts). This is true of all growing long bones (c) (Hematoxylin and Eosin, H&E a, b  $\times 20$ ; c  $\times 40$ )

are disease entities that can predispose to fractures is useful to remember, TBBD as a specific condition has not been accepted as a disease entity in the wider medical community and has been criticized in the literature (Mendelson 2007; Sprigg 2011).

Subclinical vitamin D deficiency has been offered as an explanation for fractures otherwise regarded as inflicted in young children. To date, however, studies have not found a link between vitamin D deficiency alone (in the absence of rickets) and increased fracture risk.

Chapman et al. (2010) described 40 children, age 2–24 months, with rickets. Thirty-eight of the 40 had osteopenia evident radiographically. Seven (17.5 %) of these children had fractures, and their radiographic studies demonstrated obvious rachitic changes and widespread metaphyseal fraying/cupping. None of the fractures occurred in radiographically normal bone or bone with only subtle rachitic

**Fig. 15.35** Acute posterior rib fractures in a fatally abused toddler. When the thoracic cavity is initially inspected, the only clue to injury is the blush of hemorrhage (*arrows*) beneath the parietal pleura



changes, and all of the fractures occurred in mobile infants and toddlers. No CMLs or posterior–medial rib fractures occurred. The authors concluded that their study could not support the claim that multiple fractures occur in infants with radiographically subclinical vitamin D deficiency.

Schilling et al. (2011) described 118 children younger than 2 years of age admitted to the hospital with fractures, the majority of which were accidental. Thirty-nine percent of the children had deficient or insufficient vitamin D levels. When compared to the group of children with fractures who had normal vitamin D levels, there was no association between vitamin D levels and a child abuse diagnosis, multiple fractures, rib fractures, or metaphyseal fractures.

Untreated rickets can result in dwarfism, genu valgum, bowed legs, frontal bossing, scoliosis, and fractures in severe cases. Plain radiographs show widening of the growth plate and bowing of long bones. Histologically, in addition to the globally decreased mineralization, rickets also demonstrates disordered enchondral ossification with persistence of the cartilage growth plate penetrating into the medullary cavity (Horvai and Boyce 2011) (Figs. 15.51, 15.52).

**Fig. 15.36** Stripping the pleura from the ribs in Fig. 15.35 reveals the rib fractures (*arrows*). It is incumbent upon the pathologist to actively seek such fractures since, because of their acute nature and the presence of the vertebral transverse process behind them, these fractures would likely be missed on plain film radiography (Reproduced, with permission, from Lonergan et al. (2003). From the archives of the AFIP. Child abuse: radiologic-pathologic correlation. *RadioGraphics*, 23:818)

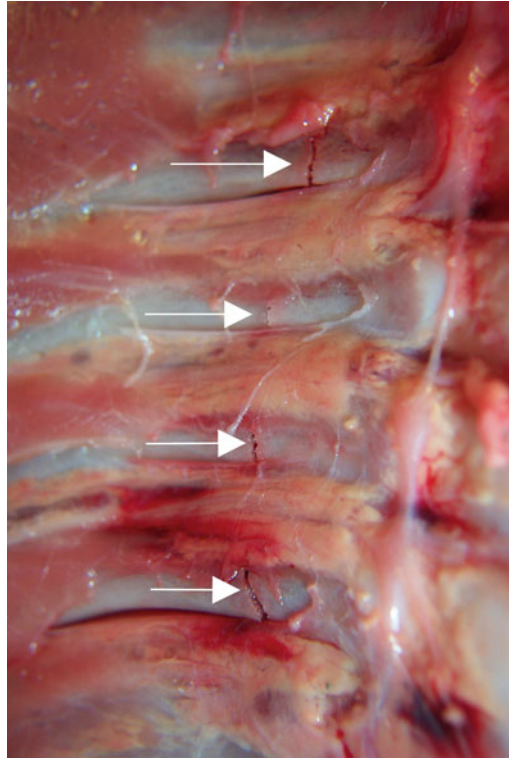
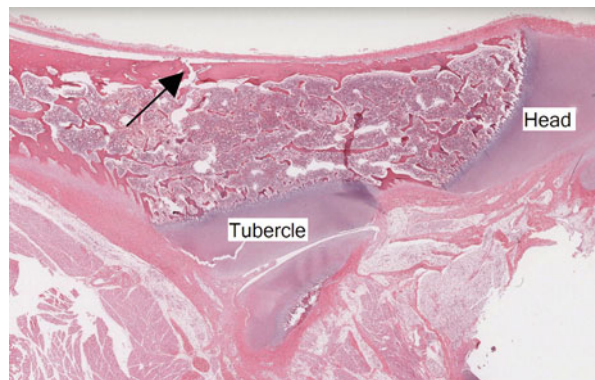


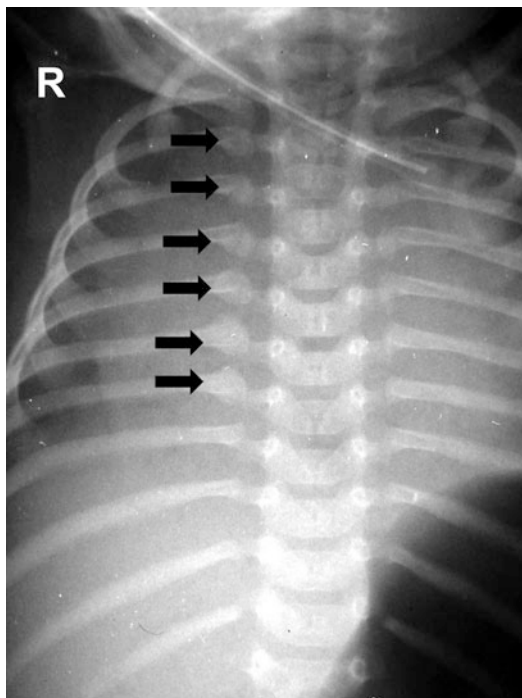
**Fig. 15.37** Histological evaluation of a fracture from Fig. 15.35 shows that only the ventral cortex (*arrow*) is fractured in this instance. As would be expected based on the mechanics of how such fractures occur, the fracture is in the head-neck-tubercle complex of the posterior rib, where the rib is levered over the transverse process of the vertebra (Hematoxylin and Eosin, H&E  $\times 1$ )



Osteogenesis imperfecta (OI) is a genetic disease caused, in most cases, by a mutation in one of the genes that encodes the  $\alpha$  chain of type 1 collagen. A number of different genetic mutations have been identified, and the disease has a wide span of clinical severity that ranges from neonatal deaths with



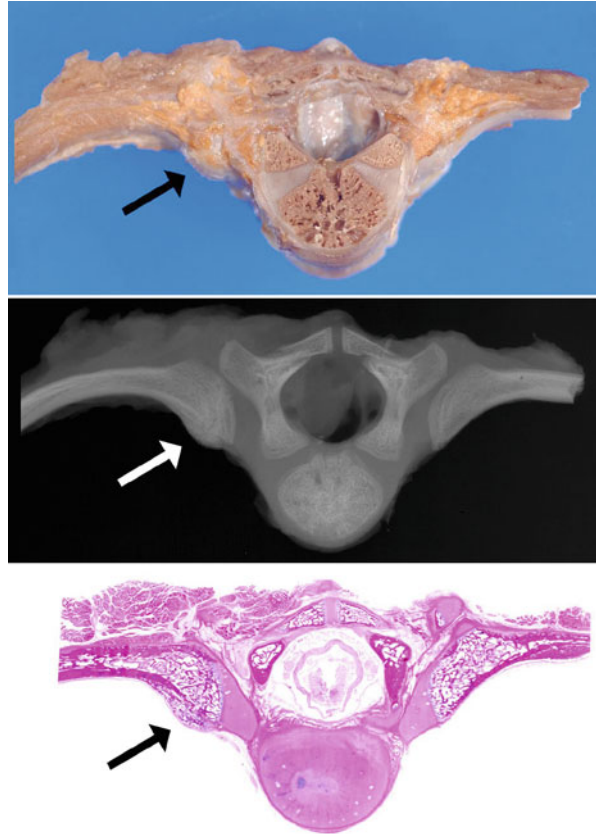
**Fig. 15.38** These healing posterior rib fractures (*arrows*) in a fatally abused infant, though plainly visible on the pre-autopsy radiograph, were missed at the time of original autopsy. Only after a subsequent infant died, also a victim of homicide, was the first child exhumed and the rib fractures photographed and evaluated (*Fig. 15.39*). Reproduced, with permission, from Lonergan et al. (2003)



numerous fractures to mild osteopenia with few fractures throughout life. Most patients fall into one of the four (I–IV) phenotypes of the Sillence classification, though other phenotypes are recognized (Rauch and Glorieux 2004). In type I, the most common and mildest form of the disease, fractures are less common than in other types and osteopenia is less severe. All patients with type I have blue sclerae. Type II is lethal and may present as stillbirth with numerous intrauterine fractures. Liveborn infants generally survive only a few weeks. Type III patients, who may have blue, gray, or white sclerae, have severe progressive disease that may result in scores of fractures before adulthood. Infants have bowed limbs. Typical radiographic features include thin cortices, widening of the metaphysis and epiphysis, and intramedullary islands of calcified cartilage. Type IV patients have disease that is intermediate in severity between types I and III. Type II and type III cases should be readily diagnosable on clinical and radiological criteria (Bishop et al. 2007). However, a small percentage of children with unexplained fractures initially thought to be inflicted may be found to have OI when tested (Marlow et al. 2002).

The histological features of bone in type I OI are osteopenia with decreased cortical thickness and trabecular volume. The architecture is normal, the bone is lamellar, and Haversian systems are present. The more severe forms of OI (II, III, IV) have an increased number of osteocytes in both cortical and trabecular bone. Another feature is

**Fig. 15.39** From Fig. 15.38, a healing posterior rib fracture (arrows) is documented grossly (*top frame*), radiographically (*middle frame*), and microscopically (*bottom frame*). As would be expected based on the mechanics of how such fractures occur, the fracture is in the head-neck-tubercle complex of the posterior rib where the rib is levered over the transverse process of the vertebra (Hematoxylin and Eosin, H&E  $\times 1$ )



the persistence of woven bone. Woven bone is most abundant in type II OI, with almost no lamellar bone. In types III and IV OI, most bone is lamellar, although some woven bone persists (McCarthy 2011). By histomorphometry, cortical bone width and cancellous bone volume are decreased in types I, III, and IV, compared to normal controls (Rauch et al. 2000) (Figs. 15.53–15.55).

## Recommendations

1. Obtain a complete skeletal survey on all deceased infants and young children that present to the medical examiner as sudden, unexpected, or unnatural deaths. The Society for Pediatric Radiology and the National Association of Medical Examiners write (Mendelson et al. 2004):



**Fig. 15.40** In situ view of healing posterior rib fractures in a fatally abused infant. Fracture calluses appear as rounded enlargements of the bone and would be expected to be visible with plain film radiography of the chest

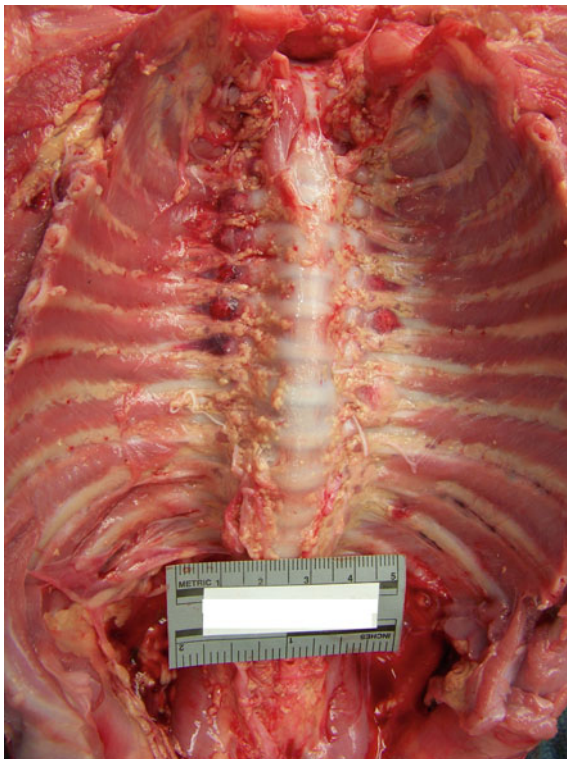


**Fig. 15.41** Gross appearance of one of the resected posterior rib fractures (*arrow*) depicted in Fig. 15.40. The fracture line is through the ventral cortex and deep into the marrow, but does not quite breach the posterior cortex



**Fig. 15.42** Whole-mount microscopy of the healing fracture in Fig. 15.41. Landmarks for orientation include the body (*B*) and transverse process (*Tr*) of the vertebra and the head (*H*)-neck (*N*)-tubercle (*T*) complex of the posterior rib. The rib periosteum (*P*) remains intact but is lifted of the ventral cortex (*C*) of the rib by fracture callus (Hematoxylin and Eosin, H&E  $\times 1$ )

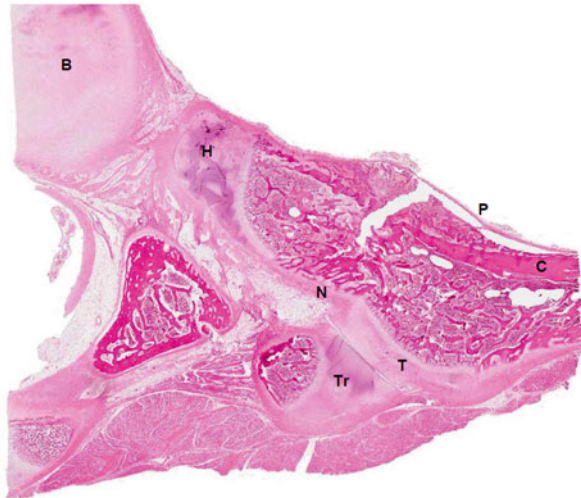


**Fig. 15.43** Higher power magnification of the fracture in Fig. 15.42 shows fracture callus composed of cartilage (*C*), woven bone (*W*), and granulation tissue (*G*). The periosteum (*P*), as is often the case with infant fractures, is lifted off the fracture by fracture callus (Hematoxylin and Eosin, H&E  $\times 40$ )

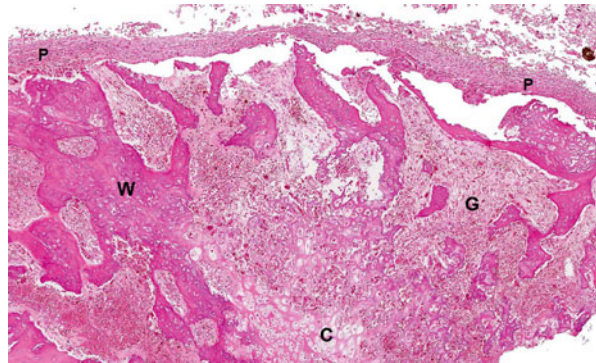


**Fig. 15.44** A posterior rib fracture viewed at low magnification (*arrow*) and higher magnification (*inset*, Hematoxylin and Eosin, H&E  $\times 20$ ). Note the mixture of tissues in the callus as well as the intact periosteum surrounding the callus (Hematoxylin and Eosin, H&E  $\times 1$ )

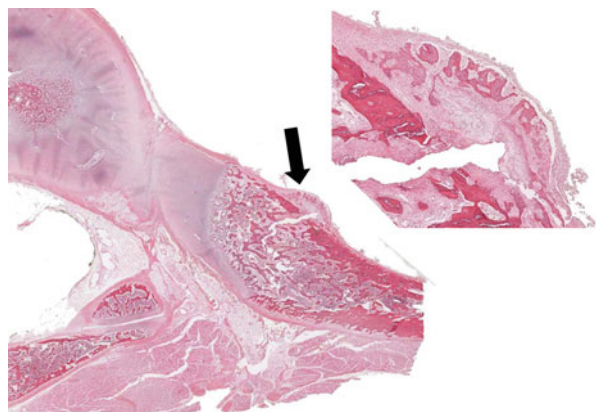


**Fig. 15.45** Healing anterior rib fractures (5–8) in a fatally battered infant. The costochondral junction can normally be quite bulbous in infants (note the appearance of ribs 3–4, which are normal). If there is any question of fracture, the concerning bones should be resected and evaluated histologically

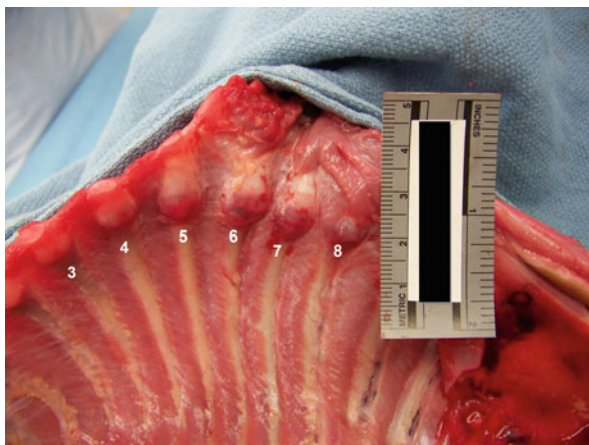


**Fig. 15.46** Radiograph of the resected costochondral junctions photographed in Fig. 15.45. The fractures (arrows) look strikingly similar to the CMLs seen on long bones of the extremities



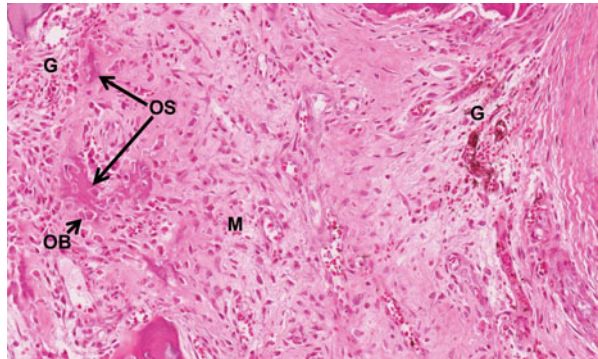
*The skeletal survey is an important component of the forensic evaluation of unexplained death that is suspicious for abuse in infants younger than 2 years of age. It may detect highly specific inflicted injuries (such as the CML) that may otherwise be missed at autopsy or during a less than complete radiographic assessment. Accurate forensic analysis of all injuries, including those documented*



**Fig. 15.47** Healing costochondral fracture from Figs. 15.45 and 15.46. The low magnification view corresponds well with the radiographic appearance, demonstrating the fracture line (\*) and the undercutting of the peripheral bone collar as the fracture approaches the outer edges of the bone (arrows) (Hematoxylin and Eosin, H&E  $\times 40$ )



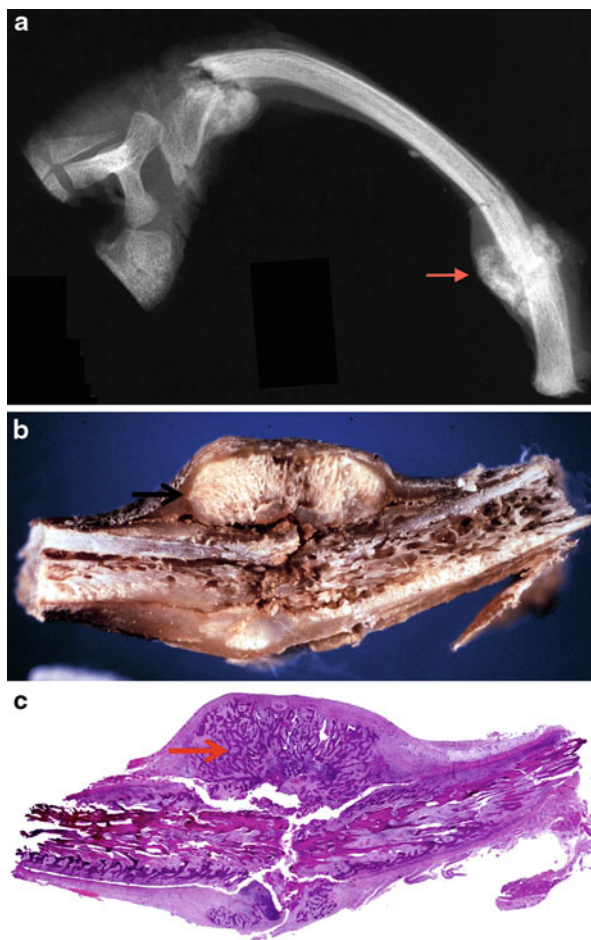
**Fig. 15.48** Healing costochondral fracture from Figs. 15.45, 15.46, and 15.47. Higher magnification shows granulation tissue (*G*) and plump mesenchymal cells (*M*) in the callus, some of which have differentiated into osteoblasts (*OB*) and begun osteoid (*OS*) production (Hematoxylin and Eosin, H&E  $\times 200$ )



*radiographically, yields the best and most thorough information about the manner and cause of death.*

- *Radiographic studies should be obtained in all unexplained deaths that are suspicious for abuse in children under 2 years of age. These should consist of, at minimum, well-collimated views of the long bones, with additional views obtained as necessary.*
- *When possible, studies should be performed by certified radiographic technicians. If this is not possible, jurisdictions need to ensure that the employees performing the studies receive adequate training. Certified radiographic facilities within the jurisdiction should make technologists available to conduct occasional training sessions where the postmortem radiographs will be obtained.*

**Fig. 15.49** (a–c) Axial radiograph (a), gross photograph (b), and whole-mount histologic section (c) of a healing rib fracture in a battered 7-week-old. Hard callus is visible radiographically, grossly, and histologically (arrows) (Hematoxylin and Eosin, H&E  $\times 1$ )



- *It is the civic responsibility of pediatric radiologists to work with the Medical Examiner/Coroner's Office in their jurisdiction to make sure that postmortem radiological examinations are optimally performed and interpreted. Professional fees, when charged, should be at a rate that would not preclude the jurisdiction from availing itself of radiological services.*
2. Always strip the pleura from the ribs to ensure that acute fractures are not missed.
  3. Resect any bones that are radiographically or grossly suspicious for acute or healing injury. It is very helpful to resect the contralateral normal bone for comparison.
  4. Resected bones should be completely fixed before they are decalcified.



**Fig. 15.50** A 5-month-old infant died of positional asphyxia in an unsafe sleeping environment. Approximately 1 month before death, he had a witnessed fall (sitting in a car seat on top of a running clothes dryer) that did not result in a discernible injury other than a right-sided scalp contusion. A linear parietal skull fracture was seen on the pre-autopsy radiographs. The specimen radiograph (*top*) shows no radiological signs of fracture healing. The largely fibrous nature of the healing process (*bottom*) bears little resemblance to the healing of long bone fractures or metaphyseal lesions. Note the absence of bone or cartilage callus (Hematoxylin and Eosin, H&E  $\times 20$ ,  $\times 40$ )

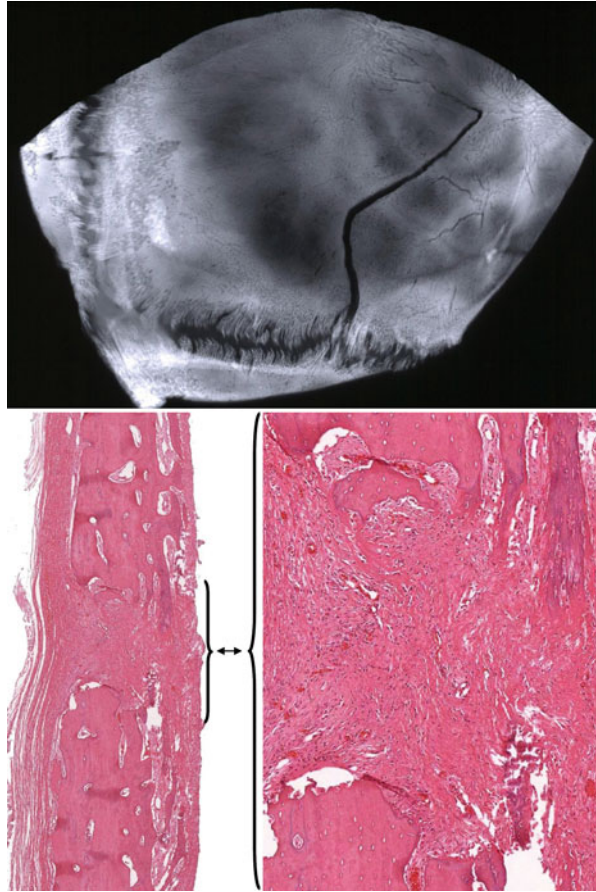


**Fig. 15.51** Rachitic costochondral junction from a 7-year-old boy. An enlarged mass of unmineralized cartilage persists in the central part of the physis (\*), with a large area of absent mineralization in the metaphysis (*brackets*) (Hematoxylin and Eosin, H&E  $\times 40$ )

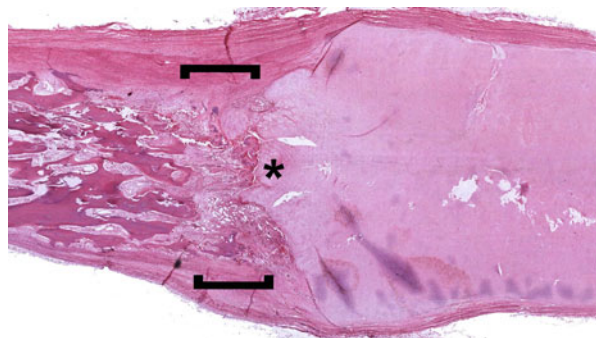


**Fig. 15.52** Higher magnification of the metaphysis of the rib in [Fig. 15.51](#). There is no normal progression of chondrocytes into the primary spongiosa, and the production of bone (\*) in the metaphysis bears little resemblance to normal bone growth (Hematoxylin and Eosin, H&E  $\times 100$ )

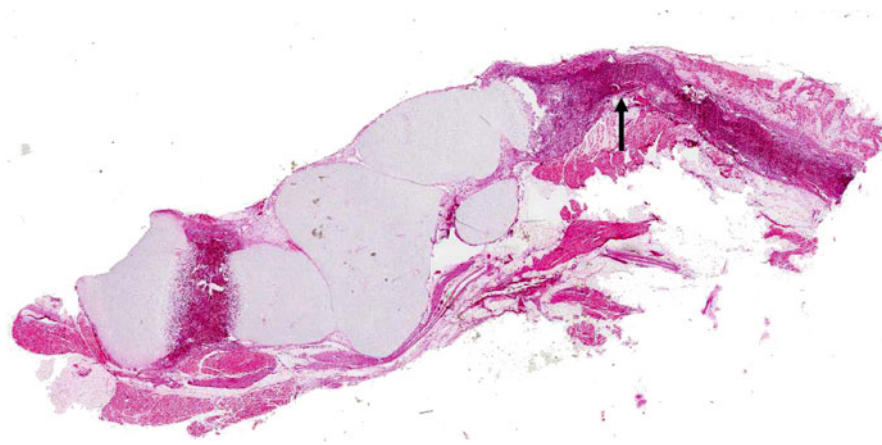
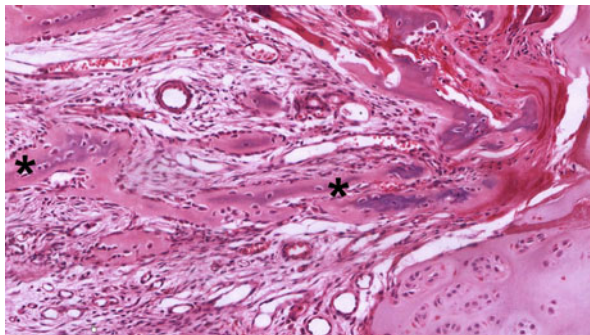


**Fig. 15.53** Distal tibia (*arrow*) in a severe case of osteogenesis imperfecta. This child died within minutes of birth. Note the extreme bowing of the bone (Hematoxylin and Eosin, H&E  $\times 1$ )

**Fig. 15.54** At higher power, the bone in [Fig. 15.53](#) has ossification at the metaphysis that is nearly absent, while woven bone in the medulla is bizarrely organized, and the cortex (\*) is largely nonexistent (Hematoxylin and Eosin, H&E  $\times 40$ )

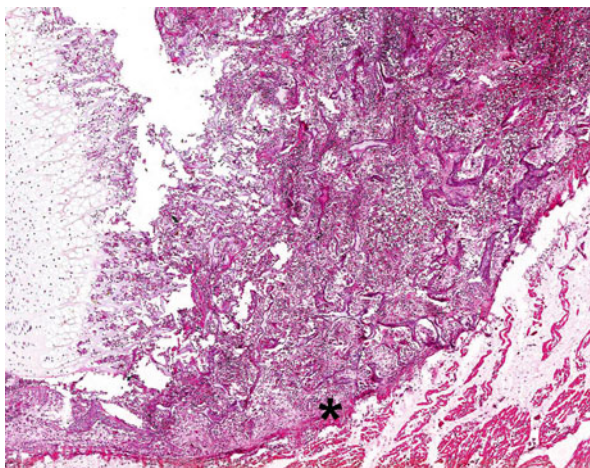
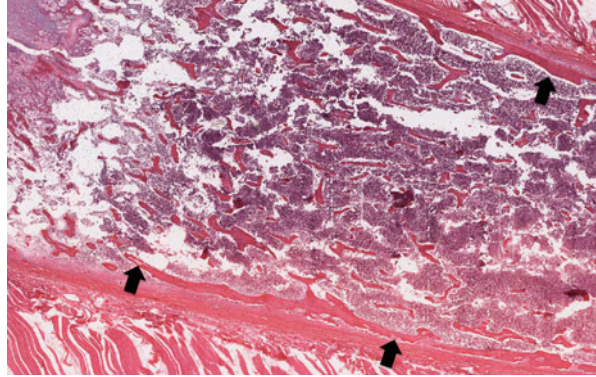


**Fig. 15.55** Longitudinal rib section from a 27-day-old with short extremities and bowed femurs who died of respiratory failure, diagnosed with osteogenesis imperfecta. The cortices (*arrows*) appear thinned and discontinuous (Hematoxylin and Eosin, H&E  $\times 100$ )



5. Decalcified bones should be carefully sectioned, ideally in the same plane as any radiographs, to allow radiological–histological correlation.
6. The features of healing of injuries should be described in the autopsy report, but be very cautious in any attempt to “date” injuries. Very little, if any, actual data exist that allow dating of bony injuries. Radiographic ability to “date” long bone injuries is also extremely limited (Halliday et al. 2011).

---

## Conclusions

- Some fractures in infants and very young children, especially posterior rib fractures and CMLs, have a very high specificity for inflicted injury.
- It is incumbent upon the pathologist to actively seek out, via radiography, gross inspection, and microscopy, fractures in the deceased child who may have been abused.
- Little data exist to meaningfully “date” fractures, though different stages of healing are readily recognized microscopically.
- Skull fracture healing bears little resemblance to the healing of diaphyseal fractures in long bones.

---

## Bibliography

- Barsness KA, Cha ES, Bensard DD, Calkins CM, Partrick DA, Karrer FM, Strain JD. The positive predictive value of rib fractures as an indicator of nonaccidental trauma in children. *J Trauma*. 2003;54:1107–10.
- Bishop N, Sprigg A, Dalton A. Unexplained fractures in infancy: looking for fragile bones. *Arch Dis Child*. 2007;92:251–6.
- Caffey J. Multiple fractures in the long bones of infants suffering from chronic subdural hematoma. *Am J Roentgenol Radium Ther Nucl Med*. 1946;56:163–73.

- Caffey J. Some traumatic lesions in growing bones other than fractures and dislocations: clinical and radiological features. *Br J Radiol.* 1957;30:225–38.
- Chapman T, Sugar N, Done S, Marasigan J, Wambold N, Feldman K. Fractures in infants and toddlers with rickets. *Pediatr Radiol.* 2010;40:1184–9.
- Clouse JR, Lantz PE. Posterior rib fractures in infants associated with cardiopulmonary resuscitation [Abstract]. American Academy of Forensic Sciences; 2008.
- Dolinak D. Rib fractures in infants due to cardiopulmonary resuscitation efforts. *Am J Forensic Med Pathol.* 2007;28:107–10.
- Duval JV, Andrew TA. Two thumb method of infant CPR: is there an increased risk for posterior rib fractures? [Abstract]. National Association of Medical Examiners; 2007.
- Halliday KE, Broderick NJ, Somers JM, Hawkes R. Dating fractures in infants. *Clin Radiol.* 2011;66:1049–54.
- Horvai AE, Boyce BF. Metabolic bone diseases. *Semin Diagn Pathol.* 2011;28:13–25.
- Hughes-Roberts Y, Arthurs OJ, Moss H, Set PAK. Postmortem skeletal surveys in suspected non-accidental injury. *Clin Radiol.* 2012;67:868–76.
- Kleinman PK. Bony thoracic trauma. In: Kleinman PK, editor. *Diagnostic imaging of child abuse.* 2nd ed. St. Louis: Mosby; 1998.
- Kleinman PK. Problems in the diagnosis of metaphyseal fractures. *Pediatr Radiol.* 2008;38 (Suppl 3):S388–94.
- Kleinman PK. The spectrum of non-accidental Injuries (child abuse) and its imitators. In: Hodler J et al., editor. *Musculoskeletal diseases 2009–2012. Diagnostic imaging 41th international diagnostic course in Davos (IDKD) Davos, March 29–April 3, 2009. Italy: Springer; 2009.*
- Kleinman PK, Marks Jr SC. A regional approach to the classic metaphyseal lesion in abused infants: the distal femur. *Am J Roentgenol.* 1998;170:43–7.
- Kleinman PK, Schlesinger AE. Mechanical factors associated with posterior rib fractures: laboratory and case studies. *Pediatr Radiol.* 1997;27:87–91.
- Kleinman PK, Marks SC, Blackbourne B. The metaphyseal lesion in abused infants: a radiologic-histopathologic study. *Am J Roentgenol.* 1986;146:895–905.
- Kleinman PK, Marks SC, Adams VI, Blackbourne BD. Factors affecting visualization of posterior rib fractures in abused infants. *Am J Roentgenol.* 1988;150:635–8.
- Kleinman PK, Marks Jr SC, Spevak MR, Belanger PL, Richmond JM. Extension of growth-plate cartilage into the metaphysis: a sign of healing fracture in abused infants. *Am J Roentgenol.* 1991;156:775–9.
- Kleinman PK, Marks SC, Spevak MR, Richmond JM. Fractures of the rib head in abused infants. *Radiology.* 1992;185:119–23.
- Kleinman PK, Marks Jr SC, Nimkin K, Rayder SM, Kessler SC. Rib fractures in 31 abused infants: postmortem radiologic-histopathologic study. *Radiology.* 1996;200:807–10.
- Loneragan GJ, Baker AM, Morey MK, Boos SC. From the archives of the AFIP. Child abuse: radiologic-pathologic correlation. *Radiographics.* 2003;23:811–45.
- Maguire S, Mann M, John N, Ellaway B, Sibert JR, Kemp AM, Welsh Child Protection Systematic Review Group. Does cardiopulmonary resuscitation cause rib fractures in children? A systematic review. *Child Abuse Negl.* 2006;30:739–51.
- Marlow A, Pepin MG, Byers PH. Testing for osteogenesis imperfecta in cases of suspected non-accidental injury. *J Med Genet.* 2002;39:382–6.
- Matshes EM, Lew EO. Two-handed cardiopulmonary resuscitation can cause rib fractures in infants. *Am J Forensic Med Pathol.* 2010;31:303–7.
- McCarthy EF. Genetic diseases of bones and joints. *Semin Diagn Pathol.* 2011;28:26–36.
- Mendelson KL. The Society for Pediatric Radiology ad hoc Committee on Child Abuse. Critical review of “temporary brittle bone disease”. *Pediatr Radiol.* 2007;35:1036–40.
- Mendelson KL. The Society for Pediatric Radiology, the National Association of Medical Examiners. Post-mortem radiography in the evaluation of unexpected death in children less than 2 years of age whose death is suspicious for fatal abuse. *Pediatr Radiol.* 2004;34:675–7.
- Miller ME. Temporary brittle bone disease: a true entity? *Semin Perinatol.* 1999;23(2):174–82.

- Miller ME. The lesson of temporary brittle bone disease: all bones are not created equal. *Bone*. 2003;33:466–74.
- Miller ME, Hangartner TN. Temporary brittle bone disease: association with decreased fetal movement and osteopenia. *Calcif Tissue Int*. 1999;64:137–43.
- Rao P, Carty H. Non-accidental injury: review of the radiology. *Clin Radiol*. 1999;54:11–24.
- Rauch F, Glorieux FH. Osteogenesis imperfecta. *Lancet*. 2004;363:1377–85.
- Rauch F, Travers R, Parfitt AM, Glorieux FH. Static and dynamic bone histomorphometry in children with osteogenesis imperfecta. *Bone*. 2000;26(6):581–9.
- Schilling S, Wood JN, Levine MA, Langdon D, Christian CW. Vitamin D status in abused and nonabused children younger than 2 years old with fractures. *Pediatrics*. 2011;127:835–41.
- Sprigg A. Temporary brittle bone disease versus suspected non-accidental skeletal injury. *Arch Dis Child*. 2011;96(5):411–3.
- Weber MA, Risdon RA, Offiah AC, Malone M, Sebire NJ. Rib fractures identified at post-mortem examination in sudden unexpected deaths in infancy (SUDI). *Forensic Sci Int*. 2009;189:75–81.